EFDA–JET–CP(10)06/15

D. Van Eester, E. Lerche, T. Johnson, T. Hellsten, J. Ongena, M.-L. Mayoral, D. Frigione, C. Sozzi, G. Calabro, M. Lennholm, P. Beaumont, T. Blackman, D. Brennan, A. Brett, M. Cecconello, I. Coffey, A. Coyne, K. Crombe, A. Czarnecka, R. Felton, M. Gatu Johnson, C. Giroud, G. Gorini, C. Hellesen, P. Jacquet, Y. Kazakov, V. Kiptily, S. Knipe, A. Krasilnikov, Y. Lin, M. Maslov, I. Monakhov, C. Noble, M. Nocente, L. Pangioni, I. Proverbio, M. Stamp, W. Studholme, M. Tardocchi, T.W. Versloot, V. Vdovin, A. Whitehurst, E. Wooldridge, V. Zoita and JET EFDA contributors

Mode Conversion Heating in JET Plasmas with Multiple Mode Conversion Layers

"This document is intended for publication in the open literature. It is made available on the understanding that it may not be further circulated and extracts or references may not be published prior to publication of the original when applicable, or without the consent of the Publications Officer, EFDA, Culham Science Centre, Abingdon, Oxon, OX14 3DB, UK."

"Enquiries about Copyright and reproduction should be addressed to the Publications Officer, EFDA, Culham Science Centre, Abingdon, Oxon, OX14 3DB, UK."

The contents of this preprint and all other JET EFDA Preprints and Conference Papers are available to view online free at www.iop.org/Jet. This site has full search facilities and e-mail alert options. The diagrams contained within the PDFs on this site are hyperlinked from the year 1996 onwards.

Mode Conversion Heating in JET Plasmas with Multiple Mode Conversion Layers

D. Van Eester[1], E. Lerche[1], T. Johnson[2], T. Hellsten[2], J. Ongena[1], M.-L. Mayoral[3], D. Frigione[4], C. Sozzi[5], G. Calabro[4], M. Lennholm[6], P. Beaumont[3], T. Blackman[3], D. Brennan[3], A. Brett[3], M. Cecconello[7], I. Coffey[3], A. Coyne[3], K. Crombe[8], A. Czarnecka[9], R. Felton[3], M. Gatu Johnson[7], C. Giroud[3], G. Gorini[5], C. Hellesen[7], P. Jacquet[3], Y. Kazakov[10], V. Kiptily[3], S. Knipe[3], A. Krasilnikov[11], Y. Lin[12], M. Maslov[13], I. Monakhov[3], C. Noble[3], M. Nocente[5], L. Pangioni[3], I. Proverbio[5], M. Stamp[3], W. Studholme[3], M. Tardocchi[5], T.W. Versloot[14], V. Vdovin[15], A. Whitehurst[3], E. Wooldridge[3], V. Zoita[16] and JET EFDA contributors*

JET-EFDA, Culham Science Centre, OX14 3DB, Abingdon, UK

[1] LPP-ERM/KMS, Association Euratom-'Belgian State', TEC Partner, Brussels, Belgium
[2]Fusion Plasma Physics, Association Euratom-VR, KTH, Stockholm, Sweden,
[3]Euratom-CCFE Fusion Association, Culham Science Centre, UK,
[4]Euratom-ENEA sulla Fusione, C. R. Frascati, Frascati, Italy,
[5]Instituto di Fisica del Plasma, EURATOM-ENEA-CNR Association, Milan, Italy,
[6]EFDA Close Support Unit, Culham Science Centre, Abingdon OX14 3DB, UK
and European Commission, B-1049 Brussels, Belgium
[7]Uppsala University, Association EURATOM-VR
[8]Department of Applied Physics, Ghent University, B-9000 Ghent, Belgium
[9]Institute of Plasma Physics and Laser Microfusion, Warsaw, Poland, Uppsala, Sweden
[10]V.N. Karazin Kharkiv National University, Kharkiv, Ukraine
[11]SRC RF Troitsk Institute for Innovating and Fusion Research, Troitsk, Russia
[12]MIT Plasma Science and Fusion Center, Cambridge, MA 02139, USA
[13]CRPP-EPFL, Association Euratom-Confédération Suisse, CH-1015 Lausanne, Switzerland
[14]FOM Institute Rijnhuizen, Association EURATOM-FOM, Nieuwegein, the Netherlands
[15]RNC Kurchatov Institute, Nuclear Fusion Institute, Moscow, Russia
[16]Association EURATOM-MEdC, National Institute for Plasma Physics, Bucharest, Romania (Footnotes)
** See annex of F. Romanelli et al, "Overview of JET Results",*
(Proc. 22 [nd] IAEA Fusion Energy Conference, Geneva, Switzerland (2008)).

Preprint of Paper to be submitted for publication in Proceedings of the
37th EPS Conference on Plasma Physics, Dublin, Ireland.
(21st June 2010 - 25th June 2010)

INTRODUCTION

Mode conversion heating has become one of the standard tools to do transport analysis and is often used in rotation experiments (see e.g. [1, 2]). It relies on the mode conversion, at the Ion-Ion Hybrid (IIH) resonance, of the Fast Wave (FW) launched by standard RF antennas, to shorter wavelength waves that are efficiently damped on electrons. The interference effect described by Fuchs et al. [3] allows to significantly enhance the mode conversion and thereby the overall RF heating efficiency when the machine and plasma parameters are chosen such that an integer number of FW wavelengths can be folded in between the High Field Side (HFS) FW cutoff and the IIH layer. This effect was already experimentally identified in (^{3}He)-D plasmas [4] and was recently tested in (^{3}He)-H JET plasmas. In the latter case, commonly referred to as an 'inverted scenario', the ion-ion hybrid layer is positioned between the antenna on the Low Field Side (LFS) and the ion-cyclotron layer of the minority ^{3}He ions while in standard – e.g. (^{3}He)-D - scenarios the ion-cyclotron layer is in between the IIH layer and the LFS. As shown in the past [5], the (^{3}He)-H scenarios require much lower ^{3}He concentrations, X[^{3}He], to reach the mode-conversion heating regime and their RF wave behavior critically depends on the plasma composition.

1. (^{3}HE)-H JET MODE CONVERSION EXPERIMENTS

The adopted RF frequency was 32.5MHz and the toroidal magnetic field was $B_0 = 3.41$T, placing the ^{3}He cyclotron layer slightly away from the centre (R = 3.16m). Dipole ($0\pi0\pi$) phasing of the RF antenna was used and 3-4MW of RF power was coupled, yielding core electron temperatures of T_{eo} = 3-4keV while the ion temperatures stayed somewhat lower (T_{io} = 2.5-3keV).

The ^{3}He concentrations referred to in this paper are estimated from visible spectroscopy light in the divertor, linking relative light intensities of given species to their relative concentrations, relying on an expression routinely adopted to control the ^{3}He injection in real time during the experiments [4]. Because of the C wall tiles, JET plasmas typically contain 1-2% of Carbon. Additionally, D being the machine's most commonly used working gas and the fact that the reported experiments were performed after a ^{4}He plasma campaign, Deuterons and ^{4}He ions released from the wall by recycling were present in all discharges. Due to the use of diagnostic D beams, the concentration of D ions (and possibly ^{4}He ions due to the NBI duct 'contamination' resulting from a change-over from D to ^{4}He beams) was further enhanced. As the location of the ion-ion hybrid layers depends on the plasma composition, experimentally found mode conversion absorption positions can be correlated to the species' concentrations via a dispersion equation study. A minimization was performed to estimate the actual plasma composition. It was found that the presence of the small quantities of C, D and ^{4}He in the plasma – in addition to the injected ^{3}He - gave rise to a supplementary mode conversion layer close to the plasma center. Being based on the intensity of the light in the divertor and not at the confluence itself, the adopted X[^{3}He] real time control expression is believed to be able to qualitatively describe the changes of X[^{3}He] but to be inaccurate quantitatively. A multiplicative correction factor of 1.6 is found via the minimization; preliminary charge-exchange recombination spectroscopy data of the ^{3}He profile provide a similar correction.

The RF power level was modulated so that the experimental power deposition profile could be

determined from the temperature response to the power steps by FFT and break-in-slope analysis (see e.g. [6]); a more global absorption efficiency estimate followed from studying the response of the plasma energy. At $f_{modulation} = {}^{4}$Hz, both the ion and electron response could be examined but the temperature response to the power modulation was partly masked by transport. At $f_{modulation}$ = 25Hz, the ion response could no longer be captured but the RF deposition on the electrons could be determined more accurately than at ^{4}Hz. The electron RF deposition profiles are represented in Figure 1. At low X[^{3}He], 2 confluence layers exist, one of which is partly hidden as the ECE diagnostic does not sample the plasma core. At higher X[^{3}He] only the more central confluence layer remains. Overall, dominant electron heating with global heating efficiencies between 30% and 70% - depending on the ^{3}He concentration - were observed in these experiments. The electron response was clear, prompt and dominant, while the ion response typically was noisier and smaller by a factor of 4-5.

Looking in detail at the response of various signals, 3 regimes could be distinguished as a function of X[^{3}He] (see Figure 2): (i) a regime at low concentration (X[^{3}He] <1.8%) at which the RF heating is efficient, (ii) a regime at intermediate concentrations (1.8<X[^{3}He]<5%) in which the RF performance is degrading and ultimately becoming very poor, and finally (iii) a good heating regime at ^{3}He concentrations beyond 6%. The latter regime was the only one in which both the neutron rate and the (D and ^{4}He) fast ion losses were significant, in spite of the fact that the scheme was intended to predominantly heat the electrons through mode conversion. The observed tails were identified as RF heated D beam particles accelerated at their Doppler-shifted cyclotron resonance (also seen in [4]). Gamma ray analysis showed that a sub-population of fast ^{4}He particles was created. Very fast ^{3}He were observed at low X[^{3}He], in agreement with earlier results, showing that at such levels of ^{3}He minority heating at the ^{3}He cyclotron layer is the dominant heating scheme [5].

At 3He concentrations beyond 6%, the heating efficiency did not critically depend on the actual concentration while at lower concentrations (X[^{3}He]<4%) a bigger excursion in heating efficiency is observed and the estimates differ somewhat from shot to shot, and depending on whether local or global signals are chosen (see Figure 3). At intermediate concentrations, the RF system was systematically struggling to couple power to the plasma. As the ^{3}He-H ion-ion hybrid layer and its associated cutoff approach the LFS plasma edge when increasing X[^{3}He], the progressively widening evanescent layer the incoming waves have to tunnel through to reach the core was held responsible for the poor RF coupling in that regime.

2. MODELING

A numerical study with the 1D TOMCAT code [8] was done to estimate the heating efficiency. It confirmed the presence of the different regimes: At low X[^{3}He], the heating efficiency is significant and on average decreasing for increasing X[^{3}He] but its exact value depends very much on the particular parameters considered. At intermediate concentrations, the ^{3}He-H confluence/cutoff pairs goes through the LFS edge and the heating efficiency is poor. At higher concentrations the heating efficiency recovers but varies much less than at low X[^{3}He]. As an example, the heating efficiency's dependence on the toroidal mode number and on X[^{3}He] are given in Figure 4.

The key to understanding the experimental and modeling results is the constructive/destructive interference phenomenon described analytically by Fuchs [3]. Kazakov et al. [7] extended Fuchs' results to the case where 2 rather than a single mode conversion layers lie in the plasma. Via the phase integral method he found that the total mode conversion coefficient is of the form $C = T_1T_2(1-T_1T_2) + 4T_1(1-T_1)(1-T_2)\sin^2\Delta\phi/2$ in which $T_{1,2}$ are the transmission factors through the individual cutoff/resonance layers and where the argument of the interference term, $\Delta\phi = 2\Phi + \Psi_2 - \Psi_1$ (the different terms corresponding to the phases of the various reflected partial waves constituting the total reflected wave field), is similar to the Fuchs result but contains a supplementary contribution $-\Psi_2$ due to the added interaction layer. The observed experimental behavior can be understood as the (in-)sensitivity of the heating efficiency to the experimental parameters through the position of the various confluence/cutoff layers. For example the HFS cutoff location – and thus F - was found to critically depend on the toroidal mode number and thus on the antenna spectrum, while the confluence and associated LFS cutoff positions – and thus Yi - are primarily dependent on the plasma composition and the density profile.

DISCUSSION & CONCLUSIONS

Recent mode conversion experiments in (^{3}He)-H JET plasmas allowed to identify the possibility to enhance the mode conversion efficiency by properly tuning the plasma parameters but equally demonstrated that such optimization becomes nontrivial when due to multiple ion species multiple mode conversion layers simultaneously occur. The experiments also underlined that although some plasma constituents may themselves not be heated by the RF waves, they can have a considerable impact on the RF heating efficiency.

ACKNOWLEDGEMENT

This work, supported by the European Communities under the contract of the Association between EURATOM and the Belgian State, was carried out within the framework of the European Fusion Development Agreement. The views and opinions expressed herein do not necessarily reflect those of the European Commission.

REFERENCES

[1]. P. Mantica et al., PRL 96, 095002 (2006)

[2]. Y. Lin, 'ICRF mode conversion flow drive in JET D-(^{3}He) plasmas and comparison with results from Alcator C-Mod', this EPS conference, paper P5.164

[3]. V. Fuchs et al., Physics of Plasmas **2** (1995) 1637–47

[4]. D. Van Eester et al., Plasma Physics and Controlled Fusion **51** (2009) 044007

[5]. M.-L. Mayoral et al., Nuclear Fusion **46** (2006) S-550–S-563

[6]. E. Lerche et al., Plasma Physics and Controlled Fusion **50** (2008) 035003

[7]. Y. Kazakov et al., 'Enhanced ICRF mode conversion efficiency in plasmas with two mode conversion layers' submitted for publication to Plasma Physics and Controlled Fusion

[8]. D. Van Eester et al., Plasma Physics and Controlled Fusion **40** (1998) 1949–1975

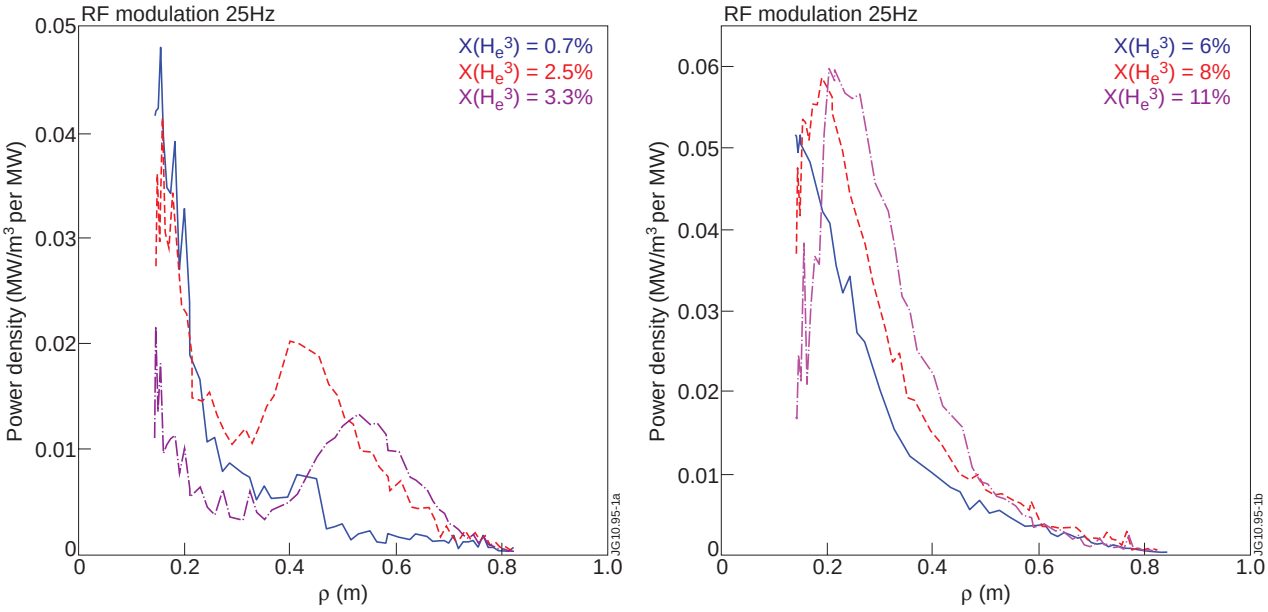

Figure 1: Electron RF power deposition profiles for various X[^{3}He]. Electron power deposition maxima identify the mode conversion loci.

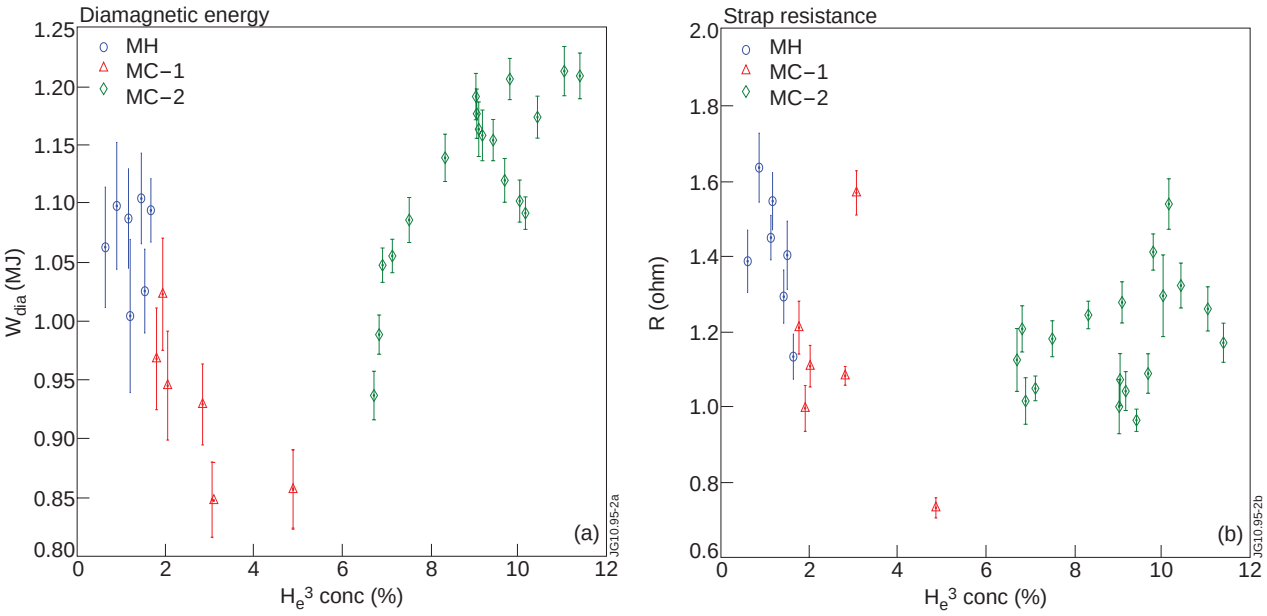

Figure 2: Dependence of (a) the diamagnetic energy and (b) the antenna resistance on X[^{3}He].

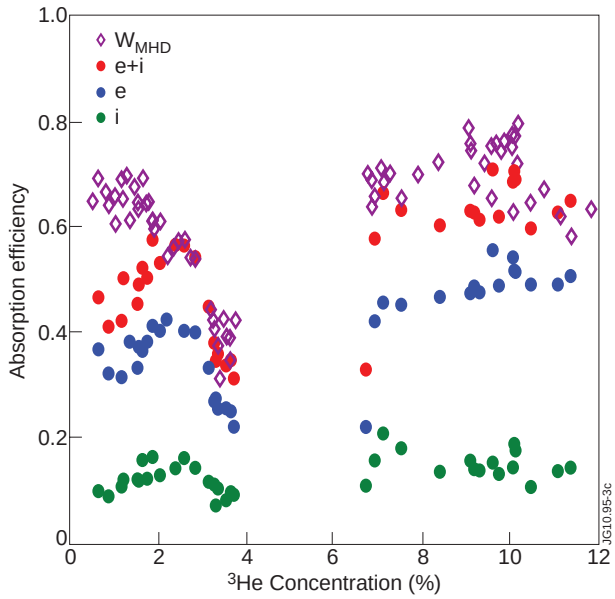

Figure 3: RF heating efficiency as a function of X[^{3}He].

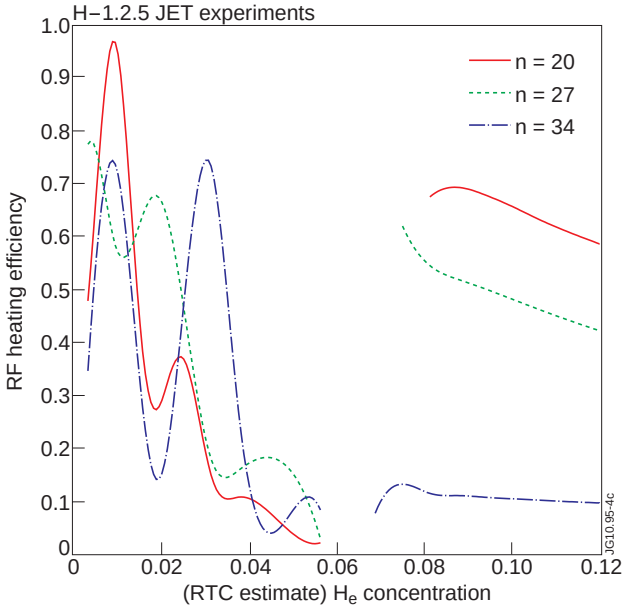

Figure 4: RF heating efficiency as a function of X[^{3}He]: sensitivity to the toroidal mode number.